

Importance of the Structure of Paper Support in Gas Transfer Properties of Protein-Coated Paper

Thibaut Cagnon, Carole Guillaume, Emmanuelle Gastaldi, Nathalie Gontard

Joint Research Unit Agropolymers Engineering and Emerging Technologies—UMR 1208 Montpellier SupAgro, INRA, UM2, CIRAD—Université Montpellier 2 CC023 place Eugène Bataillon—34095 Montpellier cedex 5, France
Correspondence to: C. Guillaume (E-mail: c-guillaume@univ-montp2.fr)

ABSTRACT: Composite materials made from fibrous support coated with agro-polymers are widely commercialized for different applications. But, their transfer properties have only been sparingly studied despite their importance in membrane technologies or food packaging. Furthermore, most of past studies on the topic have been focused on the impact of surface properties of the support on the final coated material structure and its properties; leaving unexplored the potential impact of the in-bulk structure of the support. This study demonstrated the influence of in-bulk structure and especially fibers refining degree of 4 kraft papers (SP28, 36, 60, and 80) on the structure, and surface and gas transfer properties of their respective wheat gluten (WG) coated papers (WGP28, 36, 60, and 80). Paper presenting a high fibers refining degree (SP28) exhibited very tight and narrow in bulk fibers network which prevented most of the WG-coated layer penetration, maintaining an important WG apparent layer on top of the paper and a small fibers/wheat gluten composite zone inside (WGP28). Such structure gave strong “WG-like” properties to the final coated material with moderate oxygen permeation and high permselectivity ($1.50 \times 10^{-11} \text{ mol m}^{-2} \text{ s}^{-1} \text{ Pa}^{-1}$ and 8.09, respectively for WGP28) whereas the highly impregnated structure of coated papers built on lowly refined papers (SP80, with wide and loose structure) gave coated materials presenting weak “WG-like” properties, supposedly due to a thick composite zone presenting interfacial defects, with higher oxygen permeation and very limited permselectivity ($11.90 \times 10^{-11} \text{ mol m}^{-2} \text{ s}^{-1} \text{ Pa}^{-1}$ and 1.06, respectively for WGP80).
© 2013 Wiley Periodicals, Inc. *J. Appl. Polym. Sci.* 000: 000–000, 2013

KEYWORDS: proteins; porous materials; structure–property relations; coatings

Received 15 February 2013; accepted 1 May 2013; Published online

DOI: 10.1002/app.39509

INTRODUCTION

During the last 20 years, protein-based polymers have been the focus of many studies on food packaging materials due to their low price, and their biodegradable and renewable character,^{1–3} and their unique functional properties as gases and vapor permeations.^{4,5} However, their poor mechanical properties, either too brittle at low relative humidity or not rigid enough at high relative humidity,^{5,6} needs to be improved for further industrial applications and the route of (nano-) composite materials has been already explored. Among the availability of a large range of processes and (nano-) fillers, protein based matrixes reinforced in bulk with micro^{7–10} or nanoscale^{2,8,11–18} fibrous fillers have been, by far, the most studied despite finding limited industrial applications up to now. In comparison, the yet already widely commercialized polymer-coated fibrous supports (such as papers or cardboards) have been subjected to less scientific attention and the existing studies have been mostly focused on the surface properties of these composites^{19–23} or their mechanical properties (to a lesser extent).^{23–25} Only

limited considerations have been given to their gas (O₂ and CO₂) or vapor transfer properties, which are of main interest in food packaging science considering the importance of oxygen, carbon dioxide and moisture on the preservation of food products.^{25–28} In addition, to better understand the final properties of protein coated on fibrous support, several studies have been conducted on coating and drying conditions,^{29,30} the nature of proteins,^{31,32} the chemical composition of the support,^{25,27} the surface treatment of the support.^{20,25} But surprisingly, no study has taken into consideration the impact of the structure of the support paper that is correlated to the refining degree of fibers.

This study proposes to investigate the impact of the in-bulk fibers network organization of a fibrous support on the resulting structure and gas (O₂ and CO₂) transfer and surface properties of protein-coated material. Four industrial untreated kraft papers of same chemical composition but different basis weight and pulp refining degree have been chosen as fibrous supports for coating due to their widely available character, and common use for food packaging applications (e.g., sachet for bread or

fresh fruits and vegetables). Wheat gluten (WG) have been considered for coating because of its very interesting gas transfer properties: relative humidity dependent gas transfer and surface properties and high permselectivity ratio (CO_2 permeation / O_2 permeation) at high relative humidity,⁴ especially for fruits and vegetable packaging.^{5,33,34} Four WG-coated papers were produced in identical conditions from the four different supports and their final properties (surface and gas transfer) were discussed in relation with their structure and the in-bulk structure of their respective coating support.

EXPERIMENTAL

Materials

Kraft papers (Terrana) of different basis weights 28, 36, 60, and 80 g m^{-2} (supplier data) were provided by Gascogne Paper (Mimizan, France) to serve as support papers hereinafter named Support-Papers (SP) 28, 36, 60, and 80, respectively. Samples of pastes used to process the kraft papers were also kindly provided by Gascogne Paper. Wheat gluten (WG) powder, containing 7.2 wt % of moisture and 76.5 wt % of protein was provided by Amylum (Mesnil St Nicaise, France). Acetic acid and sodium sulphite, also used to prepare the coating solution were purchased from Aldrich (St Quentin, France). Sodium dodecyl sulphate (SDS), 1,4-dithioerythritol (DTE) and iodoacetamide (IAM) for WG fractions quantification were purchased from Aldrich (St Quentin, France). For sample preparation to transmission electron microscopy, Technovit 7100 embedding kit was purchased from Labonord (Templemars, France).

WG Solution Preparation

A WG coating solution (21.23 wt %) was prepared at room temperature according to a 3-step procedure,²⁷ slightly adapted to match the desired quantities. First, 30 g of WG powder was poured into a box and dispersed under shaking in 50 mL of a sodium sulphite/deionized water solution (0.06 g/50 mL). This solution worked as a reducing agent of the disulfide bonds. Then, after 30 min of settling, the pH of the solution was set to 4 by adding a 50/50 v/v. solution of acetic acid and deionized water. Finally the solution was adjusted to 130 mL by adding deionized water and the whole mix was stirred and left to rest for a day.

WG Coating Process

Adequate procedure for coating process was determined empirically with the goal to reach a sufficient coating weight ($>10 \text{ g m}^{-2}$) and to obtain a continuous and homogenous gluten layer.

Prior to coating, all Support-Papers were stored in a relative humidity (RH) controlled box set at 30% RH. The coating was performed on the raw side of the paper at room temperature using an Erichsen coater equipped with the blade n°8 featuring a spire width of 1mm and at a speed of 10 mm s^{-1} . Three milliliters of the WG coating solution were necessary to perform the coating. These WG-coated papers will be referred hereinafter as WG-Paper (WGP) 28, 36, 60, or 80 depending on the Support-Paper coated. After coating WG-Papers were

dried slowly at room temperature and below 50% RH during 2 h.

Following the same procedure, some Support-Papers of each basis weight were also swelled by coating with acidified (pH 4) deionized water for impregnation calculation purposes.

All materials were stored at 30, 60, 90, or 100% RH and 25°C , depending on their further characterization.

Thickness Measurements

Average thicknesses of Support-Papers, swelled Support-Papers and WG-Papers were determined at room temperature and 30% RH with a hand-held digital micrometer (Mitutoyo instruments) from 10 measurements randomly taken over the paper surface.

Basis Weight and Coating Weight

To evaluate the basis weight of each Support-Paper, 9 square pieces ($5 \times 5 \text{ cm}$) of paper were cut and weighed at room temperature and 30% RH with a precision balance (Adventurer pro, Ohaus). The results were then processed to get back to the meter square scale.

To assess the coating weight, 9 square pieces ($5 \times 5 \text{ cm}$) of both Support-Paper and WG-Paper were cut and left to dry during 24 h in a ventilated oven at 103°C . They were then placed to cool into a desiccator containing silica-gel. After 1 h they were taken out and weighted with a precision balance. The coating weight (C_w) in grams per meter square was calculated as follows:

$$C_w = \frac{W_{\text{WGP}} - W_{\text{SP}}}{A} \quad (1)$$

where W_{WGP} (g) is the weight of a WG-coated paper piece, W_{SP} (g) is the average weight of Support-Paper pieces and A (m^2) is the area of a piece.

Impregnation Calculation

To evaluate the part of the WG coating solution that penetrated into the paper, the percentage of impregnation of the coated layer was calculated as follows:

$$\% \text{ Impregnation} = 100 \times \left(1 - \frac{W_{\text{Gapp}}}{e_s} \right) \quad (2)$$

where e_{WGapp} (μm) is the apparent thickness of the WG-coated layer (remaining on top of the paper) and e_s (μm) is the thickness of self-supported wheat gluten film (here present inside and on top of the paper).

e_{WGapp} was calculated from:

$$e_{\text{WGapp}} = e_{\text{WGP}} - e_{\text{SwP}} \quad (2.1)$$

where e_{WGP} (μm) is the total thickness of WG-Paper and e_{SwP} (μm) the thickness of its respective swelled paper.

e_s was determined according to the following equation previously demonstrated³²:

$$e_s = 1.6 \times C_w \quad (2.2)$$

where c_w (g m^{-2}) is the coating weight of the WG-Paper.

Microscopy Observation

Scanning Electron Microscopy. Scanning electron microscopy (SEM) observations of the paper pulps and wheat gluten-coated

papers cross sections were performed on small pieces (1×1 cm) directly mounted on stub with double-sided carbon tape. After degassing under vacuum, samples were observed with a Scanning Electron Microscope S-4800 Hitachi (Japan). All micrographs were obtained using an accelerating voltage of 2.5 kV.

Transmission Electron Microscopy. Transmission electron microscopy (TEM) observations of the WG-Papers cross-sections were performed on thin slices after embedding of the samples in Technovit epoxy resin. A transmission electron microscope H7100 from Hitachi (Tokyo, Japan) was used for observation at a voltage acceleration of 75 kV.

Wheat Gluten Fractions Quantification by SE-HPLC

Extraction of proteins and SE-HPLC analysis were performed on WG powder grinded from the apparent WG layers of each WG-Paper and on lyophilized WG powder from a control “WG casted film” (WG coating solution casted onto a Plexiglas plate following the “WG coating process procedure”). The procedure was carried out as previously described by Morel et al.,³⁵ by performing two sequential extractions. The first with a 0.1 M sodium phosphate buffer (pH 6.9) containing 1% SDS, and the second with the same buffer and a sonication step to disperse SDS-insoluble glutenin polymers. Supernatants obtained from these extractions were injected onto a size exclusion column TSK-G 4000-SW (Merck, France) (7. mm \times 30 cm) equipped with a TSK 3000-SW (Merck, France) guard column (7.5 mm, 7.5 cm). SDS-insoluble glutenin polymers (F_i) content was obtained from the total area of the chromatogram of the second extract. The contents in the other protein fractions were obtained from the first extract profile: early-eluted fractions, $F1$ and $F2$, included SDS-soluble glutenin polymers; following fractions, $F3$ and $F4$, included mainly gliadin; the last eluting fraction, $F5$, included mainly albumin and globulin. The area under the peak corresponding to each fraction was expressed in % of total protein, estimated from the sum of the total areas under the chromatograms of the two extracts, once corrected for their different solid-to-solvent ratios.³⁶ The percentage of total glutenin polymers can be calculated as the sum of F_i , $F1$, and $F2$; F_i alone gives the percentage of unextractable glutenin polymers.

Contact Angle Measurements

Wettability. Wettability of the Support-Papers was evaluated by contact angle measurement using a contact angle meter Digidrop from GBX (Bourg de Peage, France), equipped with a diffuse light source, a CDD camera (25 frames per second). The measurements were taken at 30% RH and 25°C. Prior to the measurements, the papers were cut in 5 x 50 mm bands, stuck on a glass slide using double sided adhesive and left during 2 days at the desired RH inside RH controlled chambers. The sensitivity of Support-Papers surface to wetting was investigated by measuring the behavior of a liquid drop (3 μ L) of WG coating solution, ultra-pure water and paraffin oil, onto the paper surface. Both the initial wettability and the rate of change in wettability were investigated. Wettability ($^\circ$.s⁻¹) was determined by measuring changes in averaged value of contact angles (measured on both sides of the drop) of the liquid drops with time. The evolution of volume and width basis of the drop as a

function of time were also recorded to assess the contribution of absorption (mL s⁻¹) and spreadability (mm s⁻¹) which are two phenomenon involved in wettability. All measurements were performed in triplicate.

Surface Energy. The surface energy of both Support-Papers and WG-Papers was calculated using the Owen-Wendt equation and linear regression with value of wettability equilibrium angles for diiodomethane, ultra-pure water and ethylene-glycol as entries. These wettability angles were determined via the technique described above. The Owen-Wendt equation is written as follows:

$$\gamma_L \times (1 + \cos \theta) = 2\sqrt{\gamma_L^d \times \gamma_S^d} + 2\sqrt{\gamma_L^p \times \gamma_S^p} \quad (3)$$

where θ is the angle of the drop at equilibrium in degree, θ_L the energy of the liquid phase and θ_L^d and θ_L^p its disperse and polar component and θ_S the energy of the solid phase and θ_S^d and θ_S^p its disperse and polar component. All energies are expressed in mN m⁻¹.

Wetting Envelope. The wetting envelope of a material can be determined knowing its surface's polar (θ_S^p) and disperse (θ_S^d) surface energy components. The polar and disperse fractions of the liquid (θ_L^p and θ_L^d) for which the contact angle is 0° ($\cos \theta = 1$) were calculated with the same equations after Owen-Wendt. When this polar fraction was plotted against the disperse fraction, a closed contour for $\cos \theta = 1$ was obtained. This contour was the wetting envelope, the limit between total and partial wetting of the material.

Bendtsen Roughness Measurements


The Bendtsen roughness (ISO 5636-3) of the Support-Papers was measured by Gascogne Paper (Mimizan, France) using a Bendtsen porosimeter model 6 with the entering air pressure set at 200 kPa. Five measurements were taken on each Support-Paper and the result was expressed in mL min⁻¹. Bendtsen roughness allows evaluation of the fibers refining degree of a paper: the higher the Bendtsen roughness, the lower the refining degree.

Gas Transfer Measurements

To assess the O₂ and CO₂ permeation of materials, a dynamic method using gas chromatography was used for WG-Papers and a static method using oxygen and carbon dioxide sensitive optical sensors for Support-Papers (due to high permeation of Support-Paper that saturated the gas chromatograph detector).

The O₂ and CO₂ permeation of Support-Papers were assessed in triplicate at 25°C with a static method using O₂ and CO₂ content monitoring spots and optic fibers from Presens (Regensburg, Germany).³⁷ Prior to measurements, the material was placed at the desired RH for one day to equilibrate. It was then placed on top of a permeation cell containing both one O₂ spot and one CO₂ spot situated in a RH controlled chamber (Froidlabo, France). The cell was flushed with a gas mix consisting in 50% nitrogen and 50% carbon dioxide until the amount of O₂ inside went under 1hPa and the amount of CO₂ around 5hPa. The flush was then stopped and the cell hermetically closed. The amount of O₂ and CO₂ inside the

Table I. Support Paper Structure Characterization (20°C and 30% RH)

Sample	Support paper basis weight (g m ⁻²)	Thickness of support paper (μm)	Bendtsen roughness (mL min ⁻¹)	Fiber's refining degree
SP 28	29.67 ± 0.13	40.55 ± 1.25	36.8	
SP 36	35.38 ± 0.37	49.72 ± 1.47	102	
SP 60	62.40 ± 0.38	75.68 ± 2.21	246	
SP 80	79.84 ± 1.03	92.04 ± 2.22	231	

cell was monitored via the spots and optic fibers and the permeation was calculated as follows:

$$Pe_x = \frac{J}{\Delta P \times A} \quad (4)$$

where Pe_x referred to O₂ or CO₂ permeation of the sample (mol Pa⁻¹ m⁻² s⁻¹), J the flux of gas going through the material in mole per second, ΔP to the difference in pressure exerted by the gas on each side of the film in Pascal and A to the surface of the material in meter square.

The O₂ and CO₂ permeation of WG-Papers were assessed in triplicate with an isostatic and dynamic method using gas phase chromatography at 25°C. Materials were placed in a permeation cell. The inferior and superior chambers were each spread by a 30 mL min⁻¹ flux of permeant gas (O₂ or CO₂) and vector gas (Helium) respectively. The RH of the gas flux was set thanks to a bubbling flask containing water and placed in a cryothermostat regulated at a properly chosen temperature. The differential temperature imposed between the cell and the cryothermostat permitted the establishment of the desired RH in the chamber (60 or 100%). The permeation cell was coupled to a gas chromatograph GC3800 from Varian (Les Ulis, France) equipped with an automatic valve to online analyze the evolution with time of permeant gas concentration in the superior chamber of the cell (analysis of 1 mL of sample at prescribed times). The gas chromatograph was equipped with a filled column Porapak-Q from Chrompack (Les Ulis, France) of 2 m length and 0.32 mm diameter for separating O₂ and CO₂, with thermal conductivity detector (TCD). The gas (O₂ or CO₂) permeation of the material was determined as follows in the international system unit:

$$Pe_x = \frac{\Delta Q}{\Delta t \times A \times \Delta P} \quad (5)$$

where subscript Pe_x referred to O₂ or CO₂ permeation of the sample (mol Pa⁻¹ m⁻² s⁻¹), ΔQ was the number of mol of gas that pass through the film, Δt was the time for which permeation occurs, A was the exposed film area and (ΔP) is the difference in pressure exerted by the gas on each side of the film. Gas permeation was then expressed in mol m⁻² s⁻¹ Pa⁻¹ unit. For total O₂ and CO₂ desorption and RH stabilization, materials were placed prior to measurements in the permeation cell using Helium to spread both chambers.

Calculation of WG Composite Layer Theoretical Oxygen Permeability

To calculate the theoretical WG composite layer (Figure 7, apparent WG layer + interaction zone) permeability to oxygen

($P_{O_2(WGcomp)}$), the permeability (i.e., permeation time thickness) of the Support-Papers and the WG-coated paper were first calculated by dividing their permeation value by their respective thicknesses. Then the $P_{O_2(WGcomp)}$ was calculated as follows (adapted from the conventional equation for global permeability of layered composite):

$$P_{O_2(WGcomp)} = \frac{e_{WGcomp}}{\frac{e_{WGP}}{P_{O_2(WGP)}} + \frac{e_{SP}}{P_{O_2(SP)}}} \quad (6)$$

where e_{WGcomp} , e_{WGP} , and e_{SP} are the thicknesses of the WG composite layer, the WG-Paper and the Support-Paper respectively, $P_{O_2(WGP)}$ and $P_{O_2(SP)}$ are the oxygen permeability of WG-Paper and Support-Paper respectively.

RESULTS AND DISCUSSION

Characterization of Support-Papers

In Bulk Structure. Four Terrana kraft Support-Papers of identical chemical composition but different basis weights were provided under the form of sheets: SP28, SP36, SP60, and SP80. Their basis weight varied from 29.67 g m⁻² for SP28 to 79.84 g m⁻² for SP80 together with their thickness from 40.55 μm for SP28 to 92.04 μm for SP80 and their Bendtsen roughness from 36.8 for SP28 to 231 for SP80 (Table I). Bendtsen roughness value, which relies on the ability of air to penetrate in-bulk paper, is considered as a good indicator of paper porosity and so far is related to the refining degree of fibers (the lower the Bendtsen roughness value the higher the refining degree of the fibers).³⁸ When decreasing thickness of paper produced at the industrial scale, basis weight concomitantly decreases, and pulp needs to be more refined to ensure sufficient mechanical resistance.³⁹ Higher refining implies a higher inter-fiber bonding capacity and so a better paper cohesion because of an enhanced surface fibrillation with a stronger cohesion between fibers due to the presence of many microfibrils.⁴⁰

As evidenced by SEM observations of the different paper pulps (Figure 1), SP28 and SP36 exhibited more microfibrils than SP60 and SP80, and their Bendtsen roughness was lower, suggesting a tighter and less porous in bulk structure.

This was confirmed by oxygen and carbon dioxide permeation measurements at 25°C and 100% RH (Table II): gases permeation slightly decreases with increase of the refining degree of the Support-Papers. For example SP80 was 4.4 times more permeable to O₂ and 1.7 times more permeable to CO₂ than SP28. That is in agreement with previous work on eucalyptus pulps where reduction of gases permeation was also attributed to a

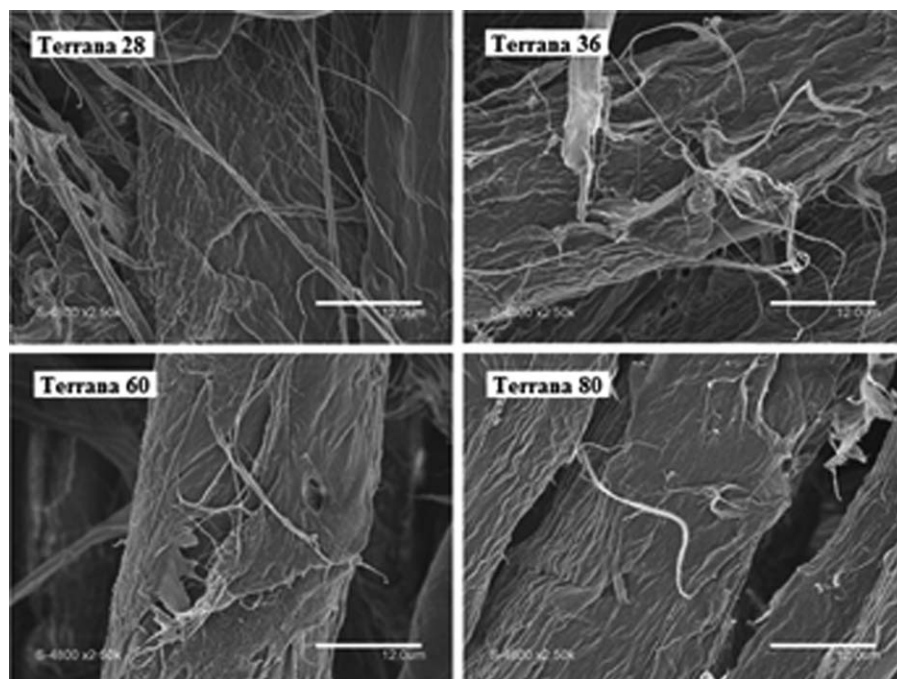


Figure 1. SEM views of Terrana Support-Papers – Impact of the refining degree on the presence of micro-fibrils (×2500).

more intricate fibers network.³⁸ It is also worth noting that all Support-Papers appeared to be somewhat less permeable to gases at moderate humidity (data not shown) than at very high humidity as previously demonstrated^{41,42}; e.g., SP28 presented a P_{eCO_2} of $0.35 \times 10^{-8} \text{ mol m}^{-2} \text{ s}^{-1} \text{ Pa}^{-1}$ at 60% RH against $9.17 \times 10^{-8} \text{ mol m}^{-2} \text{ s}^{-1} \text{ Pa}^{-1}$ at 100% RH. This is attributed to the swelling of cellulosic fibers in high RH conditions, that increases gases diffusivity.⁴¹ Whether differences in gases permeation were correlated to the different porosity of support papers, whatever the RH considered, all values remained characteristics of highly porous systems.

Surface Properties

Surface properties of the four support-papers were assessed through different contact angle measurements. First, the wetting envelope of each Support-Paper was calculated at both 60 and over 90% RH (Figure 2). No significant difference in wetting envelope was demonstrated; surface energies were circa 40 N m^{-1} at 60% RH and 33 N m^{-1} at 90% RH, whatever the Support-Paper, and the dispersive component remained higher than

the polar one whatever the RH. When RH increased, the dispersive component was slightly lowered without significantly affecting the polar one and then the hydrophobic character of papers was slightly reduced. Considering that liquid placed on the same chart is supposed to wet the material partially if outside the wetting envelope or totally if inside, Support-Papers were supposed to all be only partially wet by hydrophilic compounds such as water and partially to fully wet by hydrophobic ones such as paraffin oil. Then, droplets of the WG-coating solution, water and paraffin oil were deposited at the surface of support papers and static and dynamic contact angle measurements were performed at 30% RH and 25°C to simulate coating conditions (data not shown). Wettability (combination of absorption and spreading phenomena) of all support papers to WG coating solution and water was negligible with initial contact angle measured close to 90° and 110°, respectively. This indicated a low affinity between the Support-Papers and aqueous solution such as the WG coating solution. Initial contact angle and wettability of paraffin oil were around 30° and 10°.s⁻¹, respectively, whatever the support paper tested. As expected,

Table II. Gas Transfer Properties (P_{eO_2} , P_{eCO_2} , S) of Support-Papers and Wheat Gluten-Coated Papers at 25°C and 100% RH

Support-Papers			Wheat Gluten-coated papers			
Sample	P_{eO_2} 10 ⁻¹¹ (mol m ⁻² s ⁻¹ Pa ⁻¹)	P_{eCO_2} 10 ⁻¹¹ (mol m ⁻² s ⁻¹ Pa ⁻¹)	Sample	P_{eO_2} 10 ⁻¹¹ (mol m ⁻² s ⁻¹ Pa ⁻¹)	P_{eCO_2} 10 ⁻¹¹ (mol m ⁻² s ⁻¹ Pa ⁻¹)	S
SP 28	27900.00 ± 660.00	9170.00 ± 170.00	WGP 28	1.50 ± 0.04	12.10 ± 0.13	8.09 ± 0.27
SP 36	40800.00 ± 1780.00	5030.00 ± 140.00	WGP 36	3.35 ± 0.02	17.40 ± 0.07	5.21 ± 0.04
SP 60	43000.00 ± 0.92.00	6820.00 ± 160.00	WGP 60	8.78 ± 0.14	13.90 ± 0.35	1.58 ± 0.05
SP 80	51900.00 ± 0.65.00	6770.00 ± 140.00	WGP 80	11.80 ± 0.10	12.50 ± 0.37	1.06 ± 0.04

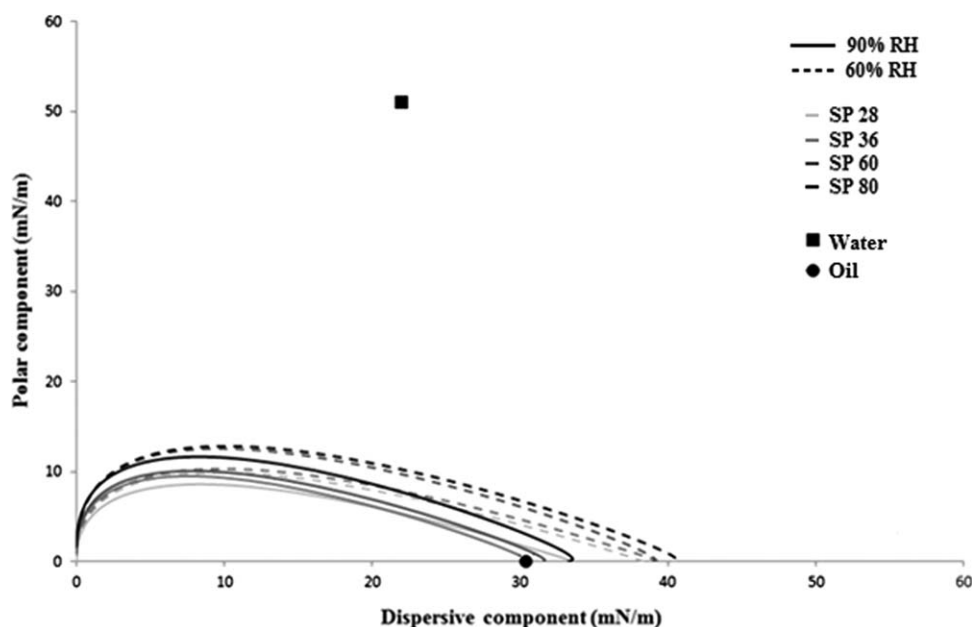


Figure 2. Wetting envelopes of the Support-Papers at 25°C and 60%RH and 90%RH.

both results confirmed that all Support-Papers were of hydrophobic nature at low RH.

With differences in fibers refining and then porosity of support papers, difference in their wettability to various liquids was also expected. Indeed the hydrophobic nature of paper has been demonstrated to be emphasized by surface roughness⁴³ which is generally correlated to the refining degree of the fibers. Thus the lowest refined papers (SP60 and SP80) were supposed to be more hydrophobic than the two others (SP36 and SP28). But, all papers used in this study were subjected to a mechanical treatment inherent to the Terrana paper production. This treatment implies friction on felt inducing folding of both fibers and micro-fibrils onto the paper surface that likely blotted out the difference in surface properties.

Structure of WG-Papers

As described in the material and method section, Support-Papers were coated with a WG solution and dried slowly at room temperature (2 h and 20°C). Depending on the basis weight of the Support-Papers, these coated materials were referred to as WG-Paper 28, 36, 60, or 80 (WGP28, 36, 60, 80).

The thicknesses of WG-Papers ranged from 62.78 to 108.17 μm , for WGP28 and WGP80, respectively. Their coating weights (C_w) were almost identical with values from 14.48 to 15.60 g m^{-2} and would lead to a WG-coated layer with a theoretical thickness around 24 μm (e_s), assuming no penetration of the layer inside the papers (Table III). TEM (Figure 3) observations of the WG-Papers cross sections evidenced the presence of a continuous WG layer in all samples. However, a significant decrease of the apparent WG layer thickness was observed with decrease of fibers refining. It should be noted that measurement of the accurate thickness of each apparent WG layer could not be performed on TEM micrographs because of the swelling induced by the preparation of samples for TEM observations (for instance, apparent thickness of WGP28 was 40 μm , much more than the maximal and theoretical value of 24 μm). SEM observations of the cross sections of the WGP were also performed and confirmed the presence of a continuous WG layer on top of every paper. As there was no swelling during preparation, measurement of the apparent thickness of this layer was possible on WGP36 and WGP60 (Figure 4). However, sample preparation was difficult and

Table III. WG-Papers Structure Characterization (20°C and 30%RH)

Sample	Coating weight (C_w) (g.m^{-2})	Theoretical thickness of apparent WG-Layer (e_s) (μm)	Thickness of WG-paper (e_{WGP}) (μm)	Thickness of respective swelled support-paper (e_{SWP}) (μm)	Thickness of apparent WG-layer (calculated) (e_{WGapp}) (μm)	Impregnation (%)
WGP 28	14.64 \pm 0.46	23.43 \pm 1.03	62.78 \pm 0.47	43.10 \pm 1.13	19.68 \pm 1.41	15.00 \pm 3.21
WGP 36	15.01 \pm 0.69	24.02 \pm 1.56	69.61 \pm 0.08	53.71 \pm 1.31	15.90 \pm 1.52	33.51 \pm 8.87
WGP 60	15.60 \pm 0.78	24.96 \pm 1.77	93.39 \pm 1.03	86.30 \pm 2.27	7.09 \pm 2.87	71.45 \pm 13.61
WGP 80	14.48 \pm 0.14	23.165 \pm 0.32	108.17 \pm 0.87	100.01 \pm 2.59	8.10 \pm 3.20	65.02 \pm 9.97

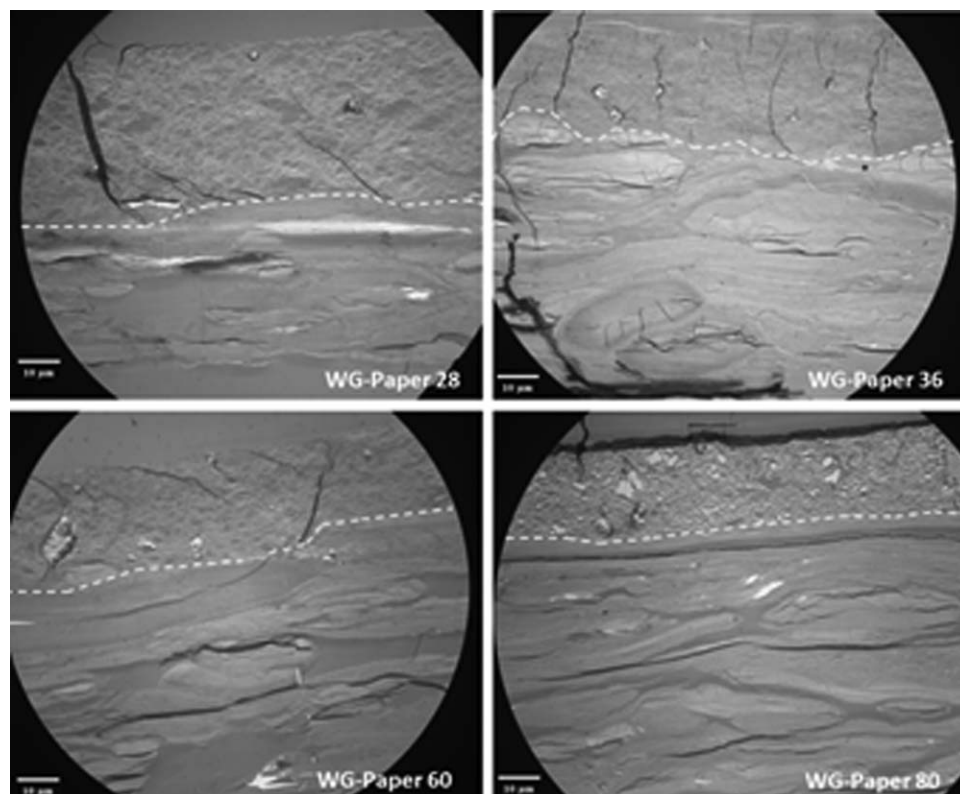


Figure 3. TEM cross-section views of the WG-Papers ($\times 1000$)—Illustration of the impact of the Support-Paper on the thickness and regularity of the WG layer. White dotted line indicates the Paper/WG separation. Note: Vertical black marks on the micrograph came from self-folding of the thin layers of material before embedding and are not representative of any potential defect on the WG-layer.

important spreading of gluten from the apparent WG layer onto the fibers was observed when cutting WGP28 and WGP80, thus no estimations were done.

To more accurately assess the apparent thickness of WG layers in each of the WG-Papers, this parameter was determined from calculation (eq. 2.2.1). Results (Table III) were coherent with SEM measurements for WGP36 and WGP60 even if they slightly differed probably because of minor WG spreading onto fibers and the local character of SEM observations. As noticed on TEM micrographs, the apparent thickness of the WG layer decreased with decrease of fibers refining and, most of all, WG layers were all thinner than the theoretical thickness ($24 \mu\text{m}$), whatever the WG paper considered. Albeit there was no affinity between

support papers and the WG coating solution during contact angle measurement, forced spreading (due to mechanical action of the coating blade) led to penetration of the coating solution into paper. This was quantified with the percentage of impregnation (eq. (2.2)) and it appeared that the higher the refining degree of the fibers, the lower the percentage of the WG-coated layer impregnated: from 15% impregnation for the WG layer of WGP28 against circa 70% for WGP60 and WGP80 (Table III). WG-papers were then all considered as tri-layered composite materials with an apparent layer of WG proteins, a composite zone with a combination of WG proteins and fibers.

Differences in impregnation of WG papers were related to the in bulk structure of their relative support papers. They were

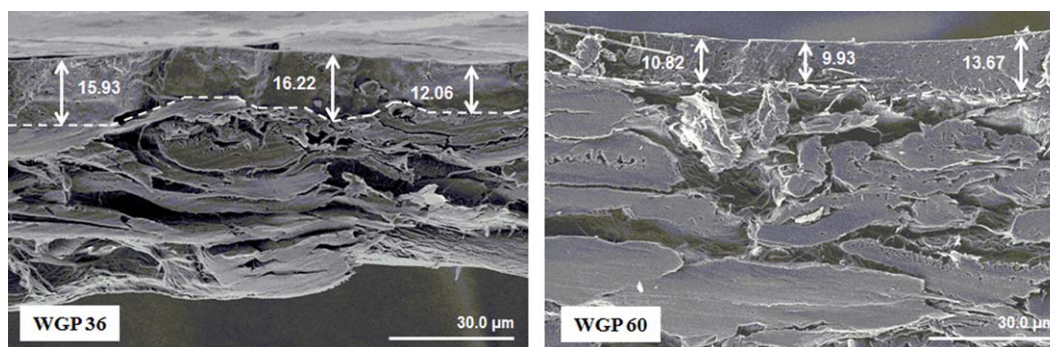


Figure 4. SEM cross-section views of the WG-Papers ($\times 1000$)—Evaluation of the thickness of the apparent WG layer. White dotted line indicates the Paper/Gluten separation.

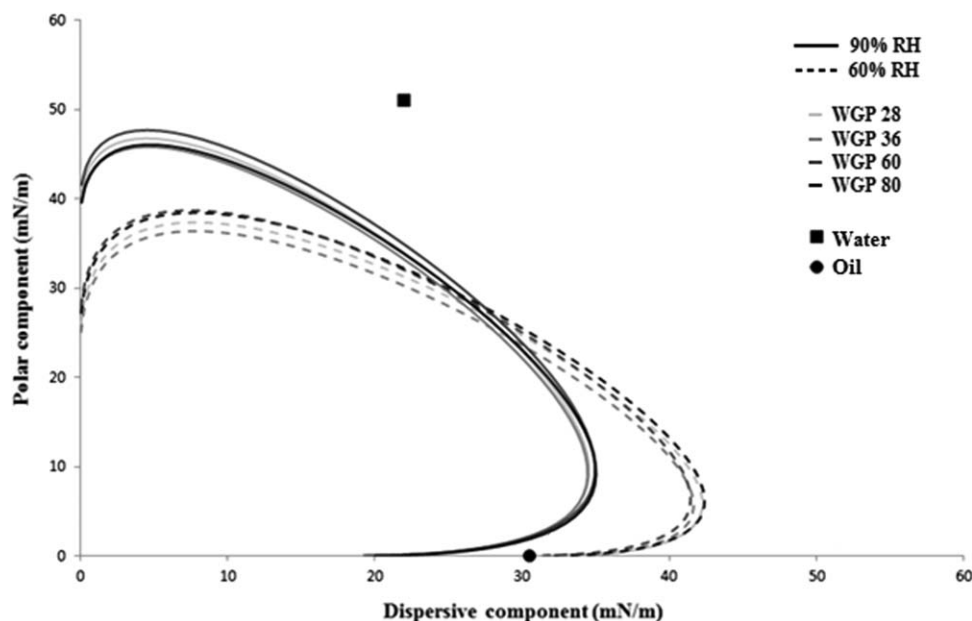


Figure 5. Wetting envelopes of the WG-Papers at 25°C and 60%RH and 90%RH.

considered as porous systems exhibiting different size of pores related to their refining degree, from a tight and narrow network in highly refined paper (as SP28) to a loose and coarse network in lowly refined paper (as SP80). After deposition at the surface of each support, WG proteins—consisting in molecules of various molecular weights (MW): glutenin polymers between 150,000 g mol^{-1} and more than 5 millions g mol^{-1} , monomeric gliadins between 17,000 and 70,000 g mol^{-1} , and then small proteins (albumin and globulin) with less than 17000 g mol^{-1} ^{44–47}—elute and split through the fibers network depending on their size (molecular weight) and/or the size of voids (pores) within the support papers. Then protein composition of the apparent layer of WG papers may be affected by this elution profile. But, no differences were observed in the protein composition of the apparent layers of the WGP. Indeed, with SE-HPLC, it was possible to determine that they all presented a composition of 1.5% high MW glutenins, 17.0% low MW glutenins, 11.5% ω -gliadins, 52.0% α - β - θ -gliadins, 14.5% albumins-globulins and 3.5% insoluble fractions which was very similar to the protein composition of a control “casted wheat gluten film”: 1.4% high MW glutenins, 13.8% low MW glutenins, 10.0% ω -gliadins, 55.7% α - β - θ -gliadins, 16.2% albumins-globulins, and 2.9% insoluble fractions. However it remains possible that a separation took place within the apparent layer with the high MW proteins remaining at the very surface of the material and the low MW proteins in the depth of the WG layer (towards the composite zone). In any case, given the differences in impregnation observed, the penetration speed of the WG coating solution was different depending on the refining degree. The lower the refining degree of the fibers (and the bigger the pore size, e.g., SP80), the faster and deeper the penetration of the coating solution (e.g., WGP80).

Surface and Gas Permeation Properties of WG-Papers Related to Their Structure

Surface Properties of WG-Papers. The surface energy of each WG-Paper was determined at 60 and over 90% RH with

different reference liquids to obtain their wetting envelopes (Figure 5). For each considered RH, no significant difference between WG-Papers was observed which was consistent with the identical apparent WG layer protein compositions observed earlier.

Whatever the humidity, surfaces of the wetting envelopes of the WG-Papers (Figure 5) were higher than those of their respective Support-Papers (Figure 2): surface energy reached 55 or 56 N m^{-1} for WG papers against 40 or 33 N m^{-1} for support papers, respectively at 60% or 90% RH. Considering the dispersive and polar components of wetting envelopes of the WG-Papers and their respective support papers, it appeared that the WG coating increased the resistance to wetting by dispersive liquids (such as oil) but decreased the resistance to polar ones (like water). This was predictable since WG films exhibit a strong hydrophilic character at the considered relative humidities.⁴⁸ It can be noted that contrary to Support-Papers, the surface properties of WG-Papers were significantly affected by the relative humidity. Despite a very similar surface energy at both 60 and 90%RH, they differed in their behavior towards polar or dispersive liquids. The WG-Papers were more sensitive to polar liquids such as water and less sensitive to dispersive ones than at 60% RH. For instance, WG-papers were totally wet by oil at 60% RH but only partially wet at 90% RH. The higher sensitivity to polar liquids was expected since WG films are known to exhibit a RH-dependent water sorption behavior characterized by an exponential shape between 60 and 100% RH, as previously evidenced.^{48,49} As a consequence, the affinity between WG-Papers and hydrophobic liquid is reduced at high RH.

Gas Transfer Properties of WG-Papers. Gases (oxygen and carbon dioxide) permeation of each WG-Paper was assessed at 25°C and 100% RH (Table II). Values, ranging from 1 to 17 $\times 10^{-11}$ $\text{mol m}^{-2} \text{s}^{-1} \text{Pa}^{-1}$ were almost in the same range than previous published data on WG-coated papers²⁷ (coating weight higher

Table IV. Calculated Gas Transfer Properties (P_{O_2} , P_{CO_2} , S) of the Composite Layer of Each WGP

Sample	RH %	Thickness composite layer (μm)	P_{O_2} composite layer 10^{-18} ($\text{mol m}^{-1} \text{s}^{-1} \text{Pa}^{-1}$)	P_{CO_2} composite layer 10^{-18} ($\text{mol m}^{-1} \text{s}^{-1} \text{Pa}^{-1}$)	S composite layer
WGP 28	60	24	278	261	0.9
WGP 28	100	24	359	2915	8.1
WGP 36	100	24	804	4181	5.2
WGP 60	100	24	2107	3342	1.6
WGP 80	100	24	2835	3015	1.1

than 20 g m^{-2}) at 80% RH, between 11×10^{-11} and $38 \times 10^{-11} \text{ mol m}^{-2} \text{ s}^{-1} \text{ Pa}^{-1}$. All WG-Papers exhibited far lower (10^3 – 10^4 times) O_2 and CO_2 permeation values than their respective Support-Paper, proving that (i) the apparent WG layer was continuous and (ii) coating weight was above the 10 g m^{-2} limit in all WG papers. Those two conditions have been previously demonstrated to be compulsory to bring enhanced barrier properties to the WG-coated materials in comparison to their supports.^{25,27}

While P_{CO_2} of WG-Papers remained quite the same whatever the WG-Paper tested at 100% RH, P_{O_2} of WG papers increased when increasing the impregnation and decreasing the thickness of the apparent WG layer: WGP60 and WGP80 presented an O_2 permeation 3 to 12 times higher than WGP36 and WGP28 (Table II). As a consequence, the permselectivity ratio was concomitantly decreased from 8 for WGP28 to 1 for WGP80. And so, only WGP28 (and to a lesser extent WGP36) presented the high permselectivity characteristic of WG materials at high RH.^{4,50,51} Furthermore, only WGP28 displayed the RH-dependent gas permeation behavior of WG materials which is marked by an increase in O_2 and CO_2 permeation together with an increase in permselectivity ratio (P_{CO_2}/P_{O_2}) when increasing RH from 60 to 100% RH.^{4,50,51} Indeed, it presented a P_{O_2} of $1.23 \times 10^{-11} \text{ mol m}^{-2} \text{ s}^{-1} \text{ Pa}^{-1}$, P_{CO_2} of $1.10 \times 10^{-11} \text{ mol m}^{-2} \text{ s}^{-1} \text{ Pa}^{-1}$, and a permselectivity ratio of 0.9 at 60% RH (data not shown) against $1.50 \times 10^{-11} \text{ mol m}^{-2} \text{ s}^{-1} \text{ Pa}^{-1}$, $12.10 \times 10^{-11} \text{ mol m}^{-2} \text{ s}^{-1} \text{ Pa}^{-1}$, 8.09, respectively, at 100% RH.

To go deeper in the understanding of the gas transfer behavior of the WG-Papers, the oxygen and carbon dioxide permeability (P_{O_2} and P_{CO_2} , permeation multiplied by thickness) of the apparent WG layer of the WGP, were calculated using eq. ((6)) for bilayer composite and assuming the composite layer presented a very permeable character, as paper (Table IV).

At 100% RH, it appeared that the P_{O_2} , P_{CO_2} , and S of the apparent WG layers were different depending on the WGP. Such results were not expected given the similar protein composition observed for every apparent WG layer. These unexpected differences could be attributed to a bias in the estimation of the real apparent and continuous WG layer thickness. Indeed, the interface between the composite zone and the apparent WG layer is likely not flat since some fibers may have penetrated into the apparent WG layer illustrated on TEM micrograph of WGP60 (Figure 6).

In case of coating on highly refined papers (e.g., WGP28), which presents a thick apparent WG layer, the impact of this

bias would remain very limited whereas in case of coating on lowly refined papers (e.g., WGP60 and WGP80), which present a very thin apparent WG layer, it would be very important, as illustrated in (Figure 7).

Such considerations may explain why the P_{O_2} of the apparent WG layer increased from $300 \times 10^{-18} \text{ mol m}^{-1} \text{ s}^{-1} \text{ Pa}^{-1}$ to $945 \times 10^{-18} \text{ mol m}^{-1} \text{ s}^{-1} \text{ Pa}^{-1}$ for WGP28 and WGP80, respectively. Consequently, for lowly refined papers, the P_{O_2} of the apparent WG layer may have been overestimated due to the presence of an important fibers/WG composite part in the thickness considered; a composite part presenting a high permeability towards oxygen due to the presence of preferential diffusion path at the fibers/WG interface. Knowing that the driving force in CO_2 permeability of WG materials is the sorption capacity,⁵⁰ the presence of fibers in the apparent WG layer may reduce the CO_2 accessibility to target amino-acid of WG.⁵⁰ As a consequence, the CO_2 permeation of WGP 60 and WGP 80 is underestimated compared with a pure WG layer. Concomitantly this bias affect the permselectivity of lowly refined coated papers and explained their weak WG-like behavior compared with the strong WG-like behavior of highly refined coated papers.

Finally the transfer properties of the apparent WG layer of the material presenting the strongest WG-like behavior, WGP28, was compared to the ones of self-supported casted WG films

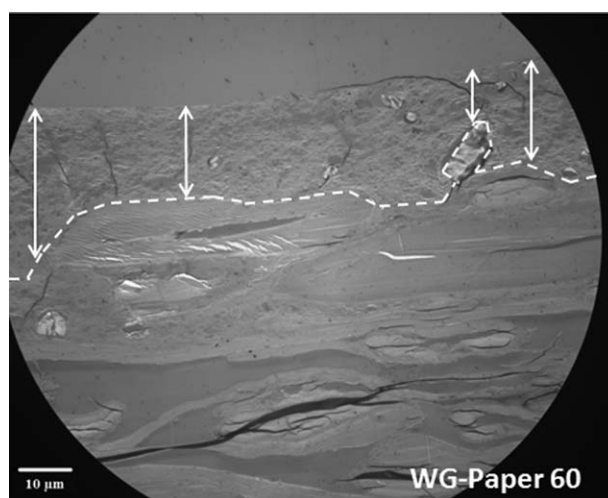


Figure 6. TEM cross-section views of the WGP60 ($\times 1000$)—Illustration of the nonflat character of the composite zone/apparent WG layer interface. White dotted line indicates the Paper/Gluten separation.

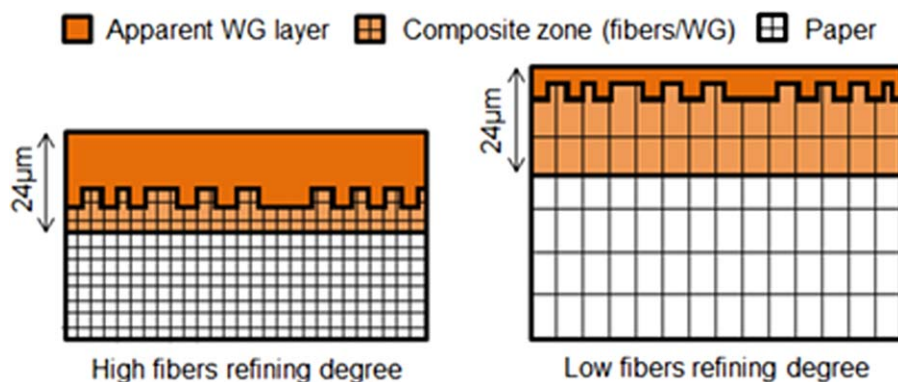


Figure 7. Schematic structure of WG-coated paper. [Color figure can be viewed in the online issue, which is available at wileyonlinelibrary.com.]

from the literature. It appeared that the RH dependent gas transfer properties were well correlated between the apparent WG layer of WGP28 and the self-supported casted WG films with a strong increase of P_{O_2} and S with RH increase from 60% to over 95% in each case. However, at 100% RH, the P_{O_2} and P_{CO_2} calculated for the apparent WG layer of WGP28 were significantly lower than the one of the self-supported casted WG film (4.3 times and 15 times lower for P_{O_2} and P_{CO_2} respectively). But these differences could easily be explained by the mandatory presence (for mechanical purposes) of glycerol inside the self-supported casted WG films that greatly enhance their permeabilities by acting as a plasticizer.^{48,52}

CONCLUSIONS

While the enhancement of gas barrier properties of paper when coated with wheat gluten (WG) proteins has been previously reported, this work brings a new understanding on the underlying mechanisms affecting structuring and consequently gas transfer properties of WG-coated paper. It appeared possible to modulate the gas transfer properties of WG coated papers (WGP) by selecting fibrous support presenting different fibers refining degrees. Increasing fibers refining led to a tighter and narrower network that would limit the penetration of the coating solution within the paper during the coating/drying process and thus reduce the impregnation of the coating solution in the support. Marginal impregnation ensured a limited thickness for the fibers/WG composite zone and the presence of a thick apparent WG layer that would bring WG-like transfer properties to the coated material. On the contrary, low fibers refining created a loose and coarse in bulk network, that led to a thick composite layer and a thin apparent WG layer and thus to a material presenting weak WG-like behavior. This principle was not considered specific to gluten coating on kraft paper and can certainly be applied to any protein coating (such as soy proteins, whey proteins, etc...) on any fibrous support (bleached pulp for instance). In addition, this way of modulating gas transfer properties could find application in packaging science, as it was the purpose here, but also in membrane sciences.

ACKNOWLEDGMENTS

The authors gratefully acknowledge the ANR for its financial support to this research through the Tailorpack project (ANR-07-

PNRA-029). The authors also thank C. Cazeville (Centre Regional d'Imagerie Cellulaire, Montpellier, France) and D. Cot (Institut Européen des Membranes, Montpellier, France) for TEM and MEB observations, respectively; and Gascogne Paper for kindly providing the industrial Support-Papers for this study.

REFERENCES

- Kumar, R.; Zhang, L. *Compos. Sci. Technol.* **2009**, *69*, 555.
- Abdul-Khalil, H. P. S.; Bhat, A. H.; Ireana Yusra, A. F. *Carbohydr. Polym.* **2012**, *87*, 963.
- Tang, X. Z.; Kumar, P.; Alavi, S.; Sandeep, K. P. *CRC Cr. Rev. Food. Sci.* **52**, 426.
- Gontard, N.; Thibault, R.; Cuq, B.; Guilbert, S. *J. Agric. Food. Chem.* **1996**, *44*, 1064.
- Cuq, B.; Gontard, N.; Guilbert, S. *Cereal Chem.* **1998**, *75*, 1.
- Gontard, N.; Guilbert, S.; Cuq, J. L. *Abstracts Papers Am. Chem. Soc.* **1992**, *204*, 217.
- Kunanopparat, T.; Menut, P.; Morel, M.-H.; Guilbert, S. *Compos. Part A: Appl. Sci. Manufac.* **2008**, *39*, 1787.
- Yu, L.; Dean, K.; Li, L. *Prog. Polym. Sci.* **2006**, *31*, 576.
- Kayserilioglu, B. S.; Bakir, U.; Yilmaz, L.; AkkaÅY, N. *Biore-sour. Technol.* **2003**, *87*, 239.
- Mastromatteo, M.; Chillo, S.; Buonocore, G. G.; Massaro, A.; Conte, A.; Del Nobile, M. A. *J. Food Eng.* **2008**, *88*, 202.
- George, J.; Siddaramaiah. *Carbohydr. Polym.* **2012**, *87* 2031–2037.
- Siro, I.; Plackett, D. *Cellulose* **2010**, *17*, 459.
- Siqueira, G.; Bras, J.; Dufresne, A. *Polymers* **2010**, *2*.
- Hubbe, M. A.; Rojas, O. J.; Lucia, L. A.; Sain, M. *Bioresour-ces* **2008**, *3*, 929.
- Chang, S.-T.; Chen, L.-C.; Lin, S.-B.; Chen, H.-H. *Food Hydrocolloid.* **2012**, *27*, 137.
- Oksman, K.; Mathew, A. P.; Bondeson, D.; Kvien, I. *Compos. Sci. Technol.* **2006**, *66*, 2776.
- Sanchez-Garcia, M. D.; Gimenez, E.; Lagaron, J. M. *Carbo-hydr. Polym.* **2008**, *71*, 235.
- Zuo, M.; Song, Y.; Zheng, Q. *J. Food Eng.* **2009**, *91*, 415.
- Andersson, C. *Packag. Technol. Sci.* **2008**, *21*, 339.

20. Trezza, T. A.; Vergano, P. J. *J. Food Sci.* **1994**, *59*, 912.
21. Han, J. H.; Krochta, J. M. *J. Food Sci.* **2001**, *66*, 294.
22. Han, J. H.; Krochta, J. M. *Trans. ASAE* **1999**, *42*, 1375.
23. Khwaldia, K.; Arab-Tehrany, E.; Desobry, S. *Comprehensive Rev. Food Sci. Food Safety* **2010**, *9*, 82.
24. Aloui, H.; Khwaldia, K.; Slama, M. B.; Hamdi, M. *Carbohydr. Polym.* **86**, 1063.
25. Gallstedt, M.; Brottman, A.; Hedenqvist, M. S. *Packag. Technol. Sci.* **2005**, *18*, 161.
26. Cagnon, T.; Guillaume, C.; Guillard, V.; Gontard, N. *Packag. Technol. Sci.* **2012**, *26*, 137.
27. Guillaume, C.; Pinte, J.; Gontard, N.; Gastaldi, E. *Food Res. Int.* **2010**, *43*, 1395.
28. Guillaume, C.; Schwab, I.; Gastaldi, E.; Gontard, N. *Innovative Food Sci. Emerging Technol.* **2010**, *11*, 690.
29. Chalier, P.; Ben Arfa, A.; Preziosi-Belloy, L.; Gontard, N. *J. Appl. Polym. Sci.* **2007**, *106*, 611.
30. Ben Arfa, A.; Preziosi-Belloy, L.; Chalier, P.; Gontard, N. *J. Agric. Food. Chem.* **2007**, *55*, 2155.
31. Chalier, P.; Tunc, S.; Gastaldi, E.; Gontard, N.; Wender, L. P.; Petersen, M. A., Control of aroma transfer by biopolymer based materials. In *Developments in Food Science*, Elsevier: **2006**; Vol. 43, p 437.
32. Gastaldi, E.; Chalier, P.; Guillemain, A.; Gontard, N. *Colloids Surfaces A: Physicochem. Eng. Aspects* **2007**, *301*, 301.
33. Barron, C.; Varoquaux, P.; Guilbert, S.; Gontard, N.; Gouble, B. *J. Food Sci.* **2002**, *67*, 251.
34. Gontard, N.; Angellier-Coussy, H.; Chalier, P.; Gastaldi, E.; Guillard, V.; Guillaume, C. S. P. Food Packaging Applications of Biopolymer-based Films. In *Biopolymers - New Materials for Sustainable Films and Coatings*; Placket, D., Eds. Wiley: Chichester, **2011**; p 213.
35. Morel, M. H.; Dehlon, P.; Autran, J. C.; Leygue, J. P.; Bar-L'Helgouac'h, C. *Cereal Chem.* **2000**, *77*, 685.
36. Morel, M. H.; Bar-L'Helgouac'h, C. In *Wheat Gluten*; Shewry, P. R.; Tatham, A. S., Eds. **2000**; p 140.
37. Penicaud, C.; Broyart, B.; Peyron, S.; Gontard, N.; Guillard, V. *J. Food Eng.* **2011**, *104*, 96.
38. Fardim, P.; Duran, N. *Colloids Surf. A: Physicochem. Eng. Aspects* **2003**, *223*, 263.
39. Bhardwaj, N. K.; Hoang, V.; Nguyen, K. L. *Bioresour. Technol.* **2007**, *98*, 1647.
40. Chevalier-Billosta, V.; Joseleau, J. P.; Cochaux, A.; Ruel, K. *Cellulose* **2007**, *14*, 141.
41. Desobry, S.; Hardy, J. *Int. J. Food Sci. Technol.* **1997**, *32*, 407.
42. Polat, O.; Crotogino, R. H.; Vanheiningen, A. R. P.; Douglas, W. J. M. *J. Pulp Pap. Sci.* **1993**, *19*, J137.
43. Quere, D. *Physica A: Stat. Mech. Appl.* **2002**, *313*, 32.
44. Lasztity, R. *Nahrung-Food* **1986**, *30*, 235.
45. Bietz, J. A.; Wall, J. S. *Cereal Chem.* **1972**, *49*, 416.
46. Morel, M. H.; Bonicel, J.; Micard, V.; Guilbert, S. *J. Agric. Food. Chem.* **2000**, *48*, 186.
47. Lagrain, B.; Goderis, B.; Brijs, K.; Delcour, J. A. *Biomacromolecules* **2010**, *11*, 533.
48. Gontard, N.; Guilbert, S.; Cuq, J. L. *J. Food Sci.* **1993**, *58*, 206.
49. Guillard, V.; Broyart, B.; Bonazzi, C.; Guilbert, S.; Gontard, N. *J. Food Sci.* **2003**, *68*, 2267.
50. Pochat-Bohatier, C.; Sanchez, J.; Gontard, N. *J. Food Eng.* **2006**, *77*, 983.
51. Mujica Paz, H.; Gontard, N. *J. Agric. Food. Chem.* **1997**, *45*, 4101.
52. Irissin-Mangata, J.; Bauduin, G. R.; Boutevin, B.; Gontard, N. *Eur. Polym. J.* **2001**, *37*, 1533.